and R. S. Wright, Aeronutronic Systems Inc. Publication No. 6-216, 1958 (unpublished).

[5]W. C. Stwalley, Phys. Rev. Lett. 37, 1628 (1976).

[6]A. J. Berlinsky, R. D. Etters, V. V. Goldman, and I. F. Silvera, Phys. Rev. Lett. 38, 356 (1977).

[7]J. T. M. Walraven, E. R. Eliel, and I. F. Silvera, Phys. Lett. 66A, 247 (1978).

[8]I. F. Silvera and J. T. M. Walraven, Phys. Lett. 74A, 193 (1979).

[9]Others have evidently also had this idea. W. C. Stwalley, in *Quantum Fluids and Solids*, edited by S. B. Trickey, E. D. Adams, and J. W. Dufty (Plenum, New York, 1977, p. 293.

[10]J. T. M. Walraven and I. F. Silvera, following Letter [Phys. Rev. Lett. 44, 168 (1980)].

[11]The necessary field for stability considered in Ref. 6 will increase for $T \neq 0$ as the pair distribution function will allow for more penetrating pair collisions as T increases.

[12]R. A. Guyer and M. D. Miller, Phys. Rev. Lett. 42, 1754 (1979).

[13]I. B. Mantz and D. O. Edwards, to be published.

[14]J. P. Toennies, W. Welz, and G. Wolf, Chem. Phys. Lett. 44, 5 (1976).

[15]For properties of these films, see, for example, J. Wilks, *The Properties of Liquid and Solid Helium* (Clarendon, Oxford 1967), Chap. 14.

[16]See Ref. 7 and references therein.

[17]S. B. Crampton, W. D. Phillips, and D. Kleppner, Bull. Am. Phys. Soc. 23, 86 (1978).

Density, Magnetization, Compression, and Thermal Leakage of Low-Temperature Atomic Hydrogen

J. T. M. Walraven and Isaac F. Silvera

Natuurkundig Laboratorium der Universiteit van Amsterdam, 1018 XE Amsterdam, The Netherlands

(Received 19 November 1979)

The density distribution of low-temperature spin-polarized atomic hydrogen in a realistic magnetic field profile is calculated for densities below and above the critical value for Bose-Einstein condensation. The distribution is an identifying characteristic. Magnetic compression and instability due to thermal leakage of the atoms is treated.

Atomic hydrogen (H) which has been shown in the accompanying Letter[1] to exist in a long-time stable state provides us with a new Bose fluid. Since in general it is necessary to prepare this gas by injecting atoms into a magnetic field, a treatment of the effect of magnetic field gradients is required. In this Letter we calculate the density distribution for spin-polarized H (H↑) in a realistic magnetic field profile. Results are obtained below and above n_c, the critical density for Bose-Einstein (BE) condensation; the effects of interactions in the high-density BE condensed state are shown to be non-negligible. The density profile is a characteristic identifying feature of the gas. This calculation immediately provides the local static magnetization, which is related to the density by a proportionality constant: the Bohr magneton. The important concept of a magnetic compression is introduced. Finally, we consider the instability of a magnetically confined gas in an open-ended container, due to thermal leakage. Comparisons are made with experiment where possible.

At low temperatures H↑ is considered to be an extremely weakly interacting Bose gas.[2] To illustrate this point we have plotted in Fig. 1 the p-V curves for H↑ at $T = 0$ K as calculated by Etters, Danilowicz, and Palmer[3] and for an ideal Bose gas at $T = 0.1$ and 0.3 K. As the 0-K curve can be looked upon as a measure of the interactions

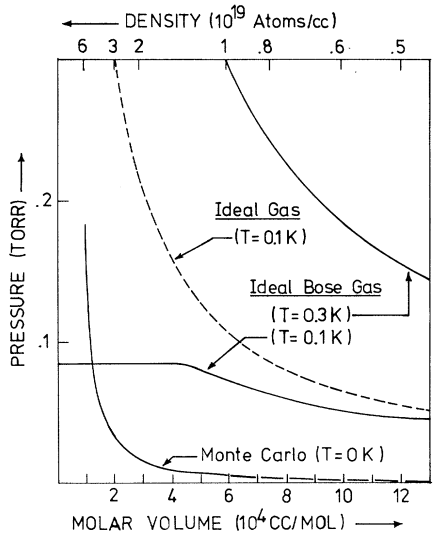

FIG. 1. p-V relation for H↑ in various approximations and at various temperatures.

within the system, no significant deviations from ideal-Bose-gas behavior are to be expected for many properties down to molar volumes and temperatures of order 10^5 cm^3/mol and 100 mK. This feature makes H↑ an ideal test probe to compare theory and experiment for a weakly interacting Bose fluid.

H↑ can only be maintained as a stable gas in a magnetic field. The confinement space (cell) must be open ended to allow loading from a source of cold atoms which can extend to zero-field regions. As a consequence the density distribution will be inhomogeneous since the field gradients exert a force on the magnetic moments of the atoms. This leads to compression of atoms in the lower two hyperfine states[4] into the high-field region, whereas the other states are repelled. We first focus our attention on the steady-state properties of H↑ in the field of a small superconducting magnet as used in the experiment described in the preceding Letter.[1] The field profile along the symmetry (z) axis is shown in Fig. 2 and is approximately quadratic over a range of 60 mm around the field maximum. Any field gradients in the xy plane are neglected since the atoms are confined to the vicinity of the z axis by means of a cylindrical tube. If we neglect

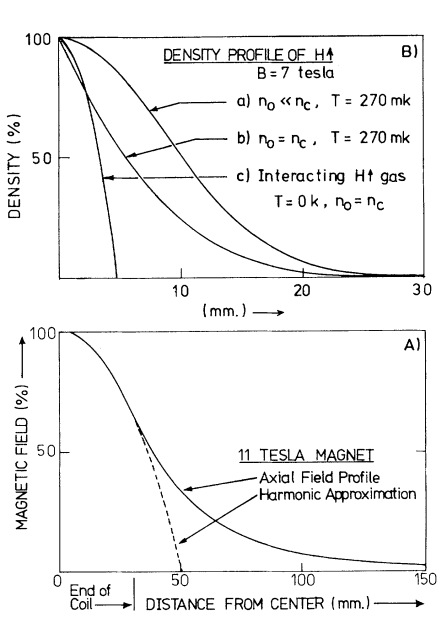

Fig. 2. (a) Magnetic field profile as a function of the distance from the center of the magnet. The end of the magnetic coil and a quadratic fit to the field are indicated. (b) Density profiles on an expanded scale. See text for explanation.

wall effects as well as all terms in the Hamiltonian beyond the electronic Zeeman term (i.e., we assume a high-field approximation), and replace the real field profile by its quadratic approximation, $B(z) = B_0[1 - (z/z_m)^2]$, the Schrödinger equation for atoms in the $m_s = -\frac{1}{2}$ electronic spin state reduces to a harmonic-oscillator (HC) problem:

$$\left[-\frac{\hbar}{2m}\nabla^2 + \mu_B B_0\left(\frac{z}{z_m}\right)^2\right]\psi = \epsilon\psi, \tag{1}$$

where m is the mass of the H atom, $2\pi\hbar$ is Planck's constant, $g = 2$ is the Landé g factor, μ_B is the Bohr magneton, B_0 is the field at the center of the magnet, and $z_m = 51$ mm in our system [see Fig. 2(a)].

The solutions of (1) are

$$\psi_{n_z\vec{k}_\perp} \sim \varphi_{n_z}(z)\exp(i\vec{k}_\perp\cdot\vec{r}_\perp), \tag{2}$$

where $\varphi_{n_z}(z)$ is a HO state and $\exp(i\vec{k}_\perp\cdot\vec{r}_\perp)$ a plane-wave state with propagation perpendicular to the symmetry axis. The energy spectrum consists of a series of bands, labeled by the HO quantum number and spaced at approximately 4×10^{-8} K. The corresponding oscillator frequency ω_0 is given by

$$\omega_0 = (2\mu_B B_0/m z_m^2)^{1/2}, \tag{3}$$

where $\omega_0 \simeq 5.5\times10^3$ rad/sec for a field of 7 T.

If one considers a *collection* of H atoms in the magnetic field, the occupation of the various states is governed by Bose statistics. As a consequence the density distribution of H↑ depends dramatically on the total number of atoms in the field as shown in Fig. 2(b). At low density (curve a) the system behaves like an ideal gas. If the density is increased the statistics lead to a compression of the gas, causing a peaking of the distribution as shown in curve b. Beyond a critical density (n_c) a "divergence" in the density occurs at the maximum field position because of the Bose condensation into the HO ground state. The classical turning points for this state are separated by 6.8 μm. However, at these densities it is no longer realistic to treat the system as an ideal Bose gas and interactions will cause the divergence to broaden as shown in curve c for $T = 0$ K.

The density distribution $n(z)$ of the gas is calculated with use of

$$n(\vec{r}) = \textstyle\sum_i W_i |\psi_i(\vec{r})|^2, \tag{4}$$

where W_i is the Bose probability for the occupation of a given state. Even at the lowest achieva-

ble temperatures many states will be occupied and as a consequence (for $n \leq n_c$) Eq. (4) can be calculated very accurately using the classical approximation for the expectation values $|\psi_i(\vec{r})|^2$ of the HO states.[5] This leads to

$$n(z) \simeq \lambda_{th}^{-3} \zeta_{3/2}(F), \tag{5}$$

where $\lambda_{th} = (2\pi\hbar^2/mkT)^{1/2}$ is the thermal wavelength,

$$\zeta_{3/2}(F) = \sum_{l=1}^{\infty} F^l/l^{3/2},$$

$$F = \exp[(\mu - \tfrac{1}{2} m\omega_0^2 z^2)kT],$$

μ is the thermodynamic potential, and k is Boltzmann's constant. $n \leq n_c$ corresponds to the condition $F \leq 1$.

The effect of the broadening of the condensate peak is estimated using the theoretical results for the ground-state energy per atom $E_1(n)$ as a function of density.[3,6] The energy to add a particle to the system is then given by

$$\mu = (\partial/\partial n)[nE_1(n)] \simeq 2an - \mu_B B \tag{6}$$

for relatively low densities, where one may write $E_1(n) = an - \mu_B B$ with $a/k = 306$ K Å.[3] Setting $n = n_c = 1.4\times10^{20}$ atoms/cm^3 at 7 T and 0.27 K one easily finds the density distribution (for the field profile under study) to depend quadratically on the distance from the center [curve c, Fig. 2(b), for $T = 0$].

In order to study the consequences of these concepts for somewhat realistic experimental conditions, consider a tube extending from zero to maximum field along the axis of a magnet. The tube is assumed to be at constant temperature and does not catalyze recombination. The zero-field density of H is maintained constant. This sets a value for the thermodynamic potential and the density can be calculated at any point using Eq. (5). It is elucidating to express this relation in terms of a compression factor, $c(z)$, and the density at maximum field: $n_0 = c(z)n(z)$. In the low-density limit

$$c(z) = \exp\{\mu_B[B_0 - B(z)]/kT\}. \tag{7}$$

The strong dependence on B and T is seen in the following examples. For the profile of Fig. 2(a) with a 7-T field at $T = 0.27$ K and $z = 40$ mm, we have $c = 8.6\times10^3$, whereas at 0.5 K, $c = 133$. For 10 T and $T = 0.1$ K, $c = 1.5\times10^{15}$.

From expression (7) we see that if, in an equilibrium condition, the density in zero field is suddenly reduced to zero (experimentally this corresponds to turning off the H discharge source), then the density n_0 in the high field must go to zero. This presents an instability for an open-ended system. The time constant for this thermal leakage in the low-density limit is found from

$$dN/dt = \int_0^{z_r} dz\, AP_1(z)\, n(z) \times \int_0^{\infty} dv_z\, P_2(v_z)\rho(v_z)v_z, \tag{8}$$

where N is the number of atoms in the field, A is the cross-sectional area of the tube, $P_1(x)$ is a geometric factor describing the probability to escape the system (pass beyond $z = z_r$) from the position z without a wall collision, $P_2(v_z) = \theta(v_z - w_z(z))$ is the probability that an atom moving in the proper direction with a velocity v_z can escape, θ is a unit step function, and

$$w_z(z) \equiv [2\mu_B(B(z) - B(z_r))/m]^{1/2}$$

is the escape velocity;

$$\rho(v_z) \equiv \alpha^{-1}\pi^{-1/2}\exp[-(v_z/\alpha)^2]$$

is the normalized velocity distribution in the z direction and $\alpha \equiv (2kT/m)^{1/2}$. Evaluating the velocity integral yields a simple rate equation, $\dot{N} = N/\tau$, where $\tau = 4cV_{eff}/K\bar{v}A$, $\bar{v} \equiv (8kT/\pi m)^{1/2}$ is the average velocity of the atoms, $V_{eff} \equiv N/n_0$, and

$$K \equiv \tfrac{1}{8}\pi^{1/2}\int_0^{z_r} P_1(z)\, dz$$

is the effective Clausing factor[7] for the system. τ is the time constant of the system. For the experiment of Ref. 1 we have calculated a time constant $\tau = 19$ msec in zero field ($V_{eff} \simeq 1.2$ cm^3) and $\tau = 110$ sec at 7 T ($V_{eff} \simeq 0.8$ cm^3), using $K = 0.1$, $\bar{v} = 100$ m/sec, and $A = 12.5$ mm^2, for magnetic compression only. The experiment yielded $\tau \simeq 1.5$ and 532 sec, respectively. We attribute the difference to additional compression due to fluxing helium vapors (HEVAC), as discussed in Ref. 1. From the experimental zero-field time constant of 1.5 sec, a HEVAC compression of 79 is estimated. In the field of 7 T the time constant due to both compressions would then be 8.7×10^3 sec (2.4 h), consistent with observations.

In summary, we stress the important result that a realistic magnetic field profile leads to a density distribution that displays macroscopic features characteristic of the Bose nature of the particles: narrowing and peaking up at the field maximum as the gas approaches the critical density. Measurement of the density or magnetization should provide a method of detecting BE con-

densation. If this state can be created, from curve c Fig. 2(b) we see that a sharp interface or "surface" in coordinate space should be a characteristic of the condensate at low temperature. At low density the gas behaves classically. The maximum density that can be loaded into a magnetic field for a gas stabilized against recombination is limited by $\exp(B/T)$ and the zero-field density.

The authors acknowledge a number of stimulating discussions on these subjects with A. J. Berlinsky, H. P. Godfried, V. V. Goldman, and A. P. M. Mattheij, as well as the financial support of the Stichting voor Fundamental Onderzoek der Materie.

[1]I. F. Silvera and J. T. M. Walraven, preceding Letter [Phys. Rev. Lett. 44, 164 (1980)].

[2]C. E. Hecht, Physica (Utrecht) 25, 1159 (1959); R. D. Etters, J. V. Dugan, and R. W. Plamer, J. Chem. Phys. 62, 313 (1975); W. C. Stwalley and L. H. Nosanow, Phys. Rev. Lett. 36, 910 (1976).

[3]R. D. Etters, R. L. Danilowicz, and R. W. Palmer, J. Low. Temp. Phys. 33, 305 (1978).

[4]N. F. Ramsey, *Molecular Beams* (Clarendon, Oxford, 1956), p. 263.

[5]L. I. Schiff, *Quantum Mechanics* (McGraw-Hill, New York, 1955), 2nd ed., p. 65.

[6]M. D. Miller and L. H. Nosanow, Phys. Rev. B 15, 4376 (1977).

[7]S. Dushman, in *Scientific Foundation of Vacuum Technique*, edited by J. M. Lafferty (Wiley, New York, 1962), 2nd ed., p. 93.

Surface-Reflectance-Spectroscopy Studies of H on W(110): Surface Band Structure and Adsorbate Geometry

Graciela B. Blanchet, P. J. Estrup, and P. J. Stiles
Department of Physics, Brown University, Providence, Rhode Island 02912
(Received 2 October 1979)

The dielectric function derived from polarized surface-reflectance-spectroscopy studies of the H/W(110) system is compared with that calculated for different hydrogen configurations. The orbital symmetry of the adsorbate states is identified and features of the surface band structure are characterized. It is found that the most likely adatom position is in a bridged site.

The determination of the electronic structure of surfaces has recently received increasing attention in both experimental and theoretical studies. In this Letter we show that surface-reflectance spectroscopy (SRS) may be a powerful tool in elucidating the relationship between the surface band structure and the adatom bonding for chemisorbed systems.

In SRS the change of reflectance caused by chemisorption on an atomically clean single-crystal surface is measured as a function of the energy of incident polarized photons.[1-4] Using this technique, we have studied the optical properties of a monolayer of hydrogen chemisorbed on tungsten(110). The results show a pronounced anisotropy in the reflectivity change which permits an investigation of the orbital character of the wave functions. Anisotropy of this type has been previously reported for O/W(110) and H/W(110) (Ref. 4) and also for Cu/Pt(110).[5]

A partial description of the surface band structure is obtained from the study of the dielectric properties that may be deduced from the reflectance spectrum. The energies of the peaks in the dielectric function[3] correspond to the excitation energies of the optical transitions and their magnitude is proportional to the dipole matrix elements between the initial- and final-state wave functions. By a change in the direction of the electric field, the matrix elements are altered either because new optical transitions are induced or because the strength of the existing ones is modified as a consequence of the directionality of the wave functions.

For each model of the adsorbate geometry there is a corresponding set of valence band orbitals. The transition matrix elements may be calculated for each model and their azimuthal dependence compared with that observed for the adsorbate peaks in the dielectric function. This type of analysis of SRS data for H/W(110) shows that bridge sites are the most probable location of the H atoms.

The experimental procedures used in SRS have been described previously.[2,3] The present study was done on a thin W(110) ribbon under ultrahigh-

